

Electronic paddle-wheels in a solid-state electrolyte

Harender S. Dhattarwal,¹ Rahul Somni,¹ and Richard C. Remsing^{1,*}

¹*Department of Chemistry and Chemical Biology, Rutgers University, Piscataway, NJ 08854*

Solid-state superionic conductors (SSICs) are promising alternatives to liquid electrolytes in batteries and other energy storage technologies. The rational design of SSICs and ultimately their deployment in battery technologies is hindered by the lack of a thorough understanding of their ion conduction mechanisms. In SSICs containing molecular ions, rotational dynamics couple to translational diffusion to create a ‘paddle-wheel’ effect that facilitates conduction. The paddle-wheel mechanism explains many important features of molecular SSICs, but an explanation for ion conduction and anharmonic lattice dynamics in SSICs composed of monatomic ions is still needed. We predict that ion conduction in the classic SSIC AgI involves ‘electronic paddle-wheels,’ rotational motion of lone pairs that couple to and facilitate ion diffusion. The electronic paddle-wheel mechanism creates a universal perspective for understanding ion conductivity in both monatomic and molecular SSICs that will create design principles for engineering solid-state electrolytes from the electronic level up to the macroscale.

Solid-state superionic conductors (SSICs) promise significant improvements over liquid electrolytes for energy storage technologies^{1–4}. Because of their use as electrolytes in solid-state batteries, SSICs have been studied extensively over the past 50 years in an effort to understand the molecular-scale principles underlying conduction^{5–7}. Conduction in molecular ionic solids is well understood. In solids like lithium sulfate, Li^+ cations rapidly diffuse through the rigid lattice made by the molecular SO_4^{2-} anions with rotational “paddle-wheel” motions of sulfate often facilitating the rapid cationic diffusion^{6,8–12}. This paddle-wheel motion has since become a principle for designing molecular SSICs^{11,13}. In contrast, similar principles have not been identified for SSICs composed of monatomic ions, like the prototypical AgI⁶, where fundamental questions concerning the coupling between the mobile cations and the immobile anionic lattice still remain^{14,15}. In this Letter, we provide new insights into the coupled cation-anion dynamics in SSICs by identifying an electronic analogue of molecular paddle-wheel motion in AgI.

Our investigation into AgI is motivated by recent ideas concerning “hidden disorder” in otherwise ordered materials. This hidden disorder is typically local and electronic in nature, arising from an interplay between electronic and nuclear degrees of freedom¹⁶. In particular, we exploit the concept of electronic plastic crystals — phases of crystalline solids in which localized lone pair electrons are dynamically orientationally disordered^{17,18}. In AgI, localized lone pairs exist on the iodide ions, and we show here that AgI is an electronic plastic crystal in its superionic phase. The rotational motion of I^- lone pair electrons accompanies the diffusion of Ag^+ through the SSIC, creating electronic paddle-wheels. This electronic paddle-wheel is summarized by the simulation snapshots in Fig. 1a, where the rotation of I^- lone pairs (light purple) facilitates the motion of an Ag^+ cation (orange) from one site to another.

Before quantifying dynamics in AgI, we first character-

ize the structural correlations involving lone pairs to identify cation coordination environments. We focus on the radial pair distribution function, $g(r)$, quantifying two-body correlations among cations, anions, and iodide lone pairs. We represent the positions of lone pairs using maximally localized Wannier function centers (MLWFCs)¹⁹, which give a reasonable description of the location of localized electron pairs. The Ag^+ -lone pair $g(r)$ exhibits two peaks at short distances, Fig. 1b. The first peak corresponds to close, direct interactions between lone pairs and Ag^+ . Integration of this peak yields a coordination number between two and three, indicating that each Ag^+ is coordinated on average by 2 or 3 sets of lone pairs. The second peak between 3 and 4 Å corresponds to correlations between the central Ag^+ and lone pairs on the iodide that are pointing away from the cation.

The coordination structure suggested by $g(r)$ is further supported through the joint probability distribution of the lone pair- Ag^+ distance (r) and the I^- -lone pair- Ag^+ angle (θ), Fig. 1c. The peak near 2 Å in $g(r)$ involves linear I^- -lone pair- Ag^+ arrangements, consistent with direct coordination of the cation by lone pair electrons. The peak near 3 Å involves values of $\theta \approx 120^\circ$, consistent with the three other tetrahedral lone pair sites of I^- pointing away from the Ag^+ . This structural analysis strongly suggests that lone pair electrons are coordinating silver cations in AgI.

In an electronic plastic crystal, lone pair electrons exhibit dynamic orientational disorder. To quantify the rotational dynamics of I^- lone pairs, we follow previous work and focus on tetrahedral rotor functions, M_γ , of order $l = 3$, such that γ labels the $(2l + 1)$ functions for each l ^{17,18,20}. The tetrahedral rotor functions do not distinguish between the four I^- MLWFCs and treat them all identically, as desired for identical electron pairs. We focus on the $\gamma = 2$ rotor function here, $M_2 = \frac{3\sqrt{5}}{40} \sum_{i=1}^4 (5x_i^3 - 3x_i r_i^2)$, where $\mathbf{r}_i = (x_i, y_i, z_i)$ is a unit vector along I-MLWFC bond i , and $r_i = |\mathbf{r}_i|$. The rotational dynamics of I^- lone pairs can be quantified

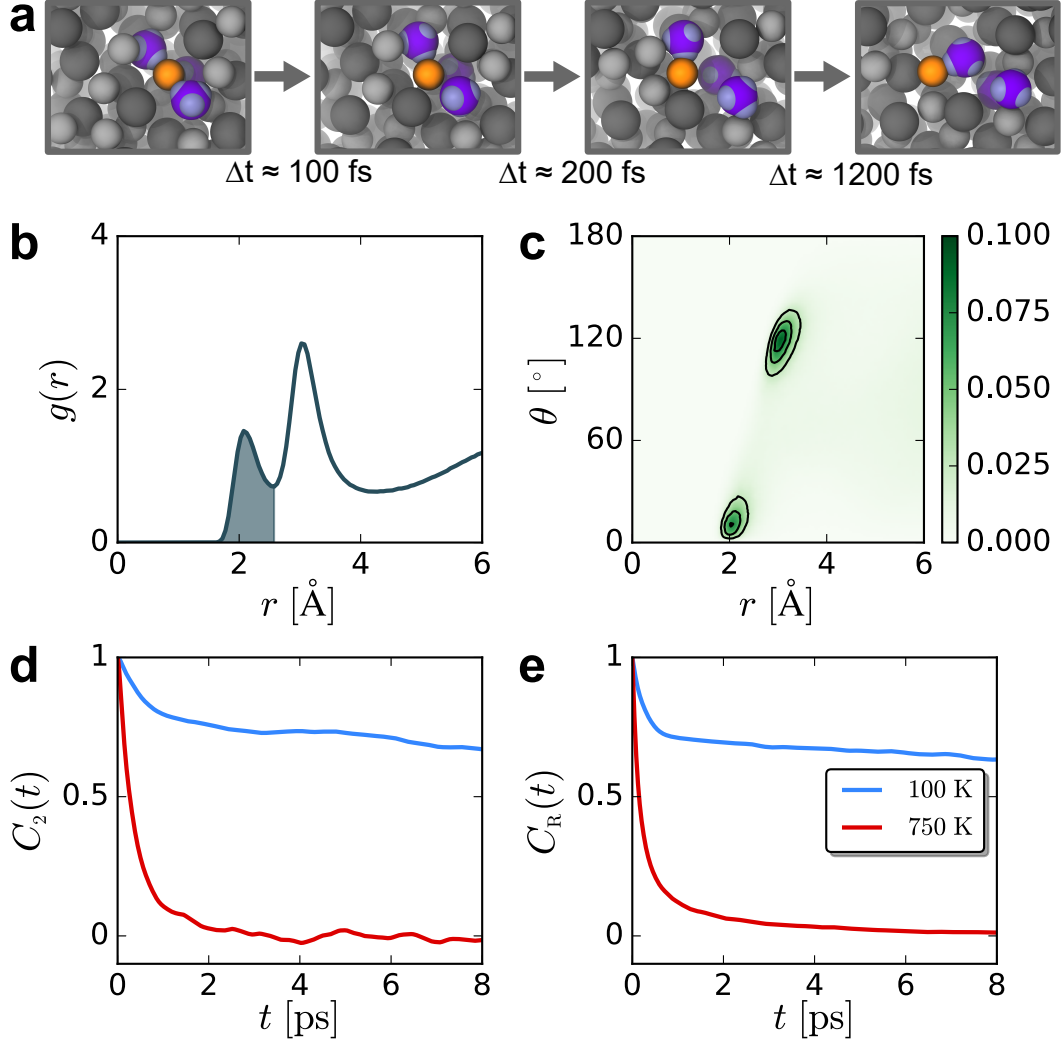


FIG. 1. (a) Snapshots from a trajectory of AgI at 750 K illustrating the electronic paddle-wheel motion that facilitates Ag^+ conduction. A single Ag^+ (orange sphere) and its initial three closest I^- (purple spheres) with their lone pair MLWFCs (small, light purple spheres) are highlighted. All other Ag^+ and I^- are shown as small gray and larger dark gray spheres. The lone pairs rotate concertedly with the motion of Ag^+ as it moves from one binding site to the next, moving from left to right along the panels shown here. Following one rotation over a 300 fs time interval, the Ag^+ stays in a binding site until it diffuses with another lone pair rotation, with the waiting time and rotation time totaling approximately 1200 fs. (b) Radial distribution functions, $g(r)$, between Ag^+ cations and iodide lone pairs, represented as maximally localized Wannier function centers. (c) Joint probability distribution of the lone pair- Ag^+ distance (r) and the I^- -lone pair- Ag^+ angle (θ). (d) Tetrahedral rotor function time correlation functions (TCFs), $C_2(t)$, characterizing I^- lone pair rotational dynamics. (e) Ag^+ cage TCF, $C_R(t)$, quantifying the diffusion of cations between binding sites.

through the time correlation function

$$C_\gamma(t) = \frac{\langle M_\gamma(0)M_\gamma(t) \rangle}{\langle M_\gamma^2(0) \rangle}, \quad (1)$$

where $\langle \dots \rangle$ indicates an ensemble average. In the superionic phase of AgI at 750 K, the rotational TCF $C_2(t)$ decays with a relaxation time of approximately 0.4-0.5 ps, indicating that MLWFC rotational motion occurs on a picosecond timescale, Fig. 1d. In comparison, similar MLWFC rotations in cesium tin halide perovskites occur

on faster timescales of 0.04-0.1 ps^{17,18}.

When Ag^+ diffuses between the various sites in the AgI lattice, the identity of the iodides making up its coordination cage changes. Therefore, we quantify Ag^+ dynamics through a TCF that probes these changes in coordination cage, inspired by the cage correlation functions used in the study of supercooled liquids²¹. We define two indicator functions, $h_i^{\text{out}}(0, t) = \Theta(1 - \xi_i^{\text{out}}(0, t))$ and $h_i^{\text{in}}(0, t) = \Theta(1 - \xi_i^{\text{in}}(0, t))$, where $\Theta(x)$ is the Heav-

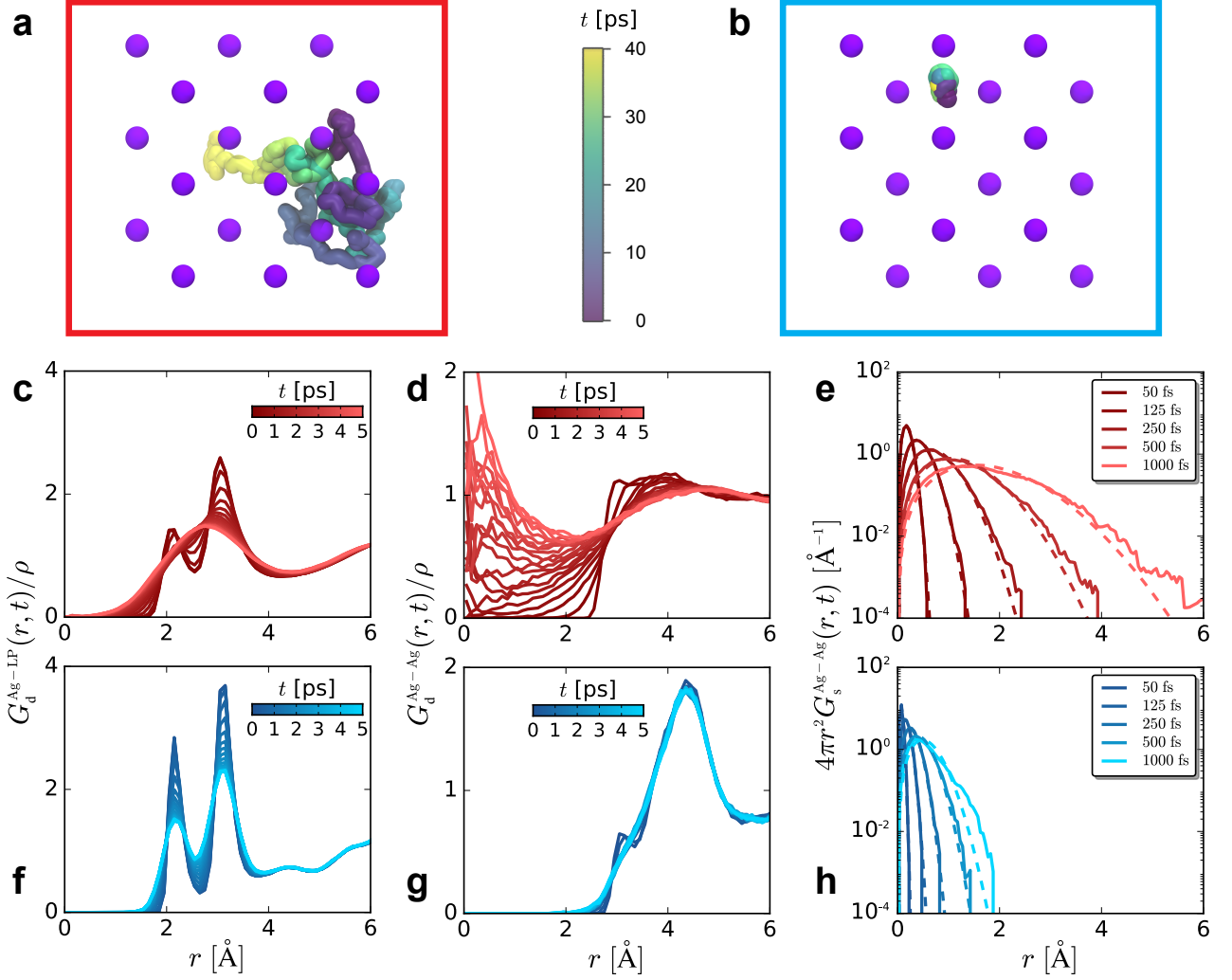


FIG. 2. Snapshots showing the trajectory of a single Ag^+ at (a) 750 K and (b) 100 K, where the Ag^+ is colored by time according to the color bar, and iodides are shown as purple spheres. The space-time dynamics in the system are quantified through the distinct van Hove correlation function for cation-lone pair correlations at (c) 750 K and (f) 100 K, the distinct van Hove correlation function for cation-cation correlations at (d) 750 K and (g) 100 K, all normalized by the bulk density, ρ , and the self van Hove correlation function for cation correlations at (e) 750 K and (h) 100 K.

iside step function,

$$\xi_i^{\text{out}}(0, t) = \frac{\ell_i(0) \cdot \ell_i(t)}{\ell_i(0) \cdot \ell_i(0)}, \quad (2)$$

$$\xi_i^{\text{in}}(0, t) = \frac{\ell_i(0) \cdot \ell_i(t)}{\ell_i(t) \cdot \ell_i(t)}, \quad (3)$$

and $\ell_i(t)$ is the neighbor list of the i th Ag^+ at time t . Therefore, $h_i^{\text{out/in}}(0, t) = 1$ if the neighbors are the same at times t and 0. If the number of neighbors decreases, then $h_i^{\text{out}}(0, t) = 0$ and $h_i^{\text{in}}(0, t) = 1$. If the number of neighbors increases, then $h_i^{\text{in}}(0, t) = 0$ and $h_i^{\text{out}}(0, t) = 1$. We then define a cage TCF as $C_R(t) = \langle h_i^{\text{out}}(0, t) h_i^{\text{in}}(0, t) \rangle$, which quantifies the diffusion of Ag^+

between occupation sites through changes in its coordination cage, like the motion shown in Fig. 1a. The cage TCF has a relaxation time of approximately 0.6-0.7 ps at 750 K, Fig. 1e, which is on a similar timescale to lone pair rotations. The similar timescales for Ag^+ diffusion out of a binding site and lone pair rotations suggests a coupling between electron rotational motion and cation diffusion.

The MLWFC rotational dynamics are temperature dependent, Fig. 1d. At the low temperature of 100 K, where AgI is no longer conductive (see SI), lone pair rotational dynamics are significantly slowed and AgI is no longer in an electronic plastic crystal phase. As a result, the lone pair rotation TCF, $C_2(t)$, and the TCF quantifying Ag^+ diffusion, $C_R(t)$, both decay very little on the timescale

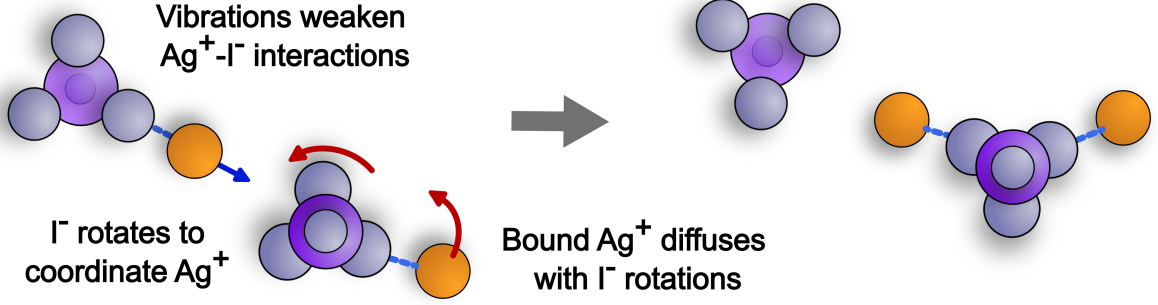


FIG. 3. Schematic diagram of the collective diffusion mechanism of Ag^+ in AgI. Thermal vibrational motion weakens some cation-anion interactions, new cation-anion interactions are formed through lone pair rotation, and these lone pair rotations are coupled to the diffusion of a coordinated Ag^+ .

of the simulations. This slowing of lone pair rotations and Ag^+ diffusion upon cooling suggests that they are intimately connected; Ag^+ cannot diffuse unless I^- lone pairs rotate.

To characterize cation diffusion in more detail, we computed the distinct and self parts of the van Hove correlation function, $G_d(r, t)$ and $G_s(r, t)$, respectively, defined according to

$$G_d(r, t) = \left\langle \frac{1}{N} \sum_i \sum_{j \neq i} \delta(|\mathbf{r}_i(0) - \mathbf{r}_j(t)|) \right\rangle \quad (4)$$

and

$$G_s(r, t) = \left\langle \frac{1}{N} \sum_i \delta(|\mathbf{r}_i(0) - \mathbf{r}_i(t)|) \right\rangle. \quad (5)$$

The distinct van Hove function, $G_d(r, t)$, quantifies space-time correlations of the initial position of one particle (i) with other particles in the system (j). The self van Hove function, $G_s(r, t)$, quantifies space-time correlations of a particle with its own initial position. For $t = 0$, $G_d(r, 0)$ is equal to the $g(r)$ between the two particle types of interest, and $G_s(r, 0)$ is a delta function at $r = 0$.

The distinct van Hove function for cation-lone pair correlations suggests electronic paddle-wheels in the SSIC phase of AgI, Fig. 2c,f. At $t = 0$, $G_d(r, t)$ is the Ag^+ -MLWFC pair distribution function. As t increases at $T = 750$ K, the first peak in $G_d(r, t)$ broadens on the timescale of paddle-wheel motion, indicating that Ag^+ and the MLWFCs are correlated. This correlation in cation and lone pair dynamics is reflective of electronic paddle-wheels. At low temperatures, when AgI is not a SSIC, $G_d(r, t)$ hardly changes shape, reflecting a lack of cation diffusion and anion lone pair rotation.

Cation motion in traditional molecular SSICs often occurs through discrete hops induced by paddle-wheel motion of molecular anions. Cations rattle in a binding site and then very rapidly move to another site during a

hop. In contrast, we find that Ag^+ dynamics are diffusive in AgI. The Ag^+ trajectories shown in Fig. 2a show no evidence of the rapid jumps indicative of hopping; the trajectories are smooth and diffusive.

The diffusive nature of cation dynamics in AgI at 750 K is further supported by $G_d(r, t)$ and $G_s(r, t)$ shown in Fig. 2d,e, while a lack of dynamics is suggested by those for AgI at 100 K, Fig. 2g,h. At $t = 0$, the cationic $G_d(r, t)$ is equal to the Ag-Ag $g(r)$. As time progresses, a peak smoothly grows in near $r = 0$, the initial location of a Ag^+ . This peak at the origin at later times is consistent with a cation leaving its initial location and another cation taking its place. The smooth growth of this peak with time suggests a lack of hopping-like motion. A similar lack of hopping can be observed in $G_s(r, t)$, Fig. 2e. Hopping manifests in $G_s(r, t)$ through the appearance of well-defined peaks at typical hopping distances. Peaks are not observed in the cation $G_s(r, t)$ and we instead find smooth distributions. However, the motion is not purely diffusive, which would result in the dashed Gaussian distributions. The deviations from Gaussian diffusion suggest that the dynamics are collective and dynamically heterogeneous, with some ions moving slower and faster than Gaussian expectations. Collective cation dynamics can be expected, because a cation cannot diffuse to another binding site unless another cation leaves that site.

The mechanism of collective dynamics in AgI is suggested by our simulations, and it involves a combination of translational and rotational dynamics. We propose three main contributions that may occur nearly simultaneously, shown in Fig. 3. Thermally-induced translational fluctuations weaken the strength a Ag^+ - I^- interaction. The Ag^+ is then coordinated by a different I^- , and the newly coordinating I^- rotates its lone pairs to form this new interaction. The rotating I^- coordinates other cations, and one of these coordinated cations diffuses by accompanying the lone pair rotation.

The diffusive dynamics of the Ag^+ cations observed here represents a fundamental difference between electronic paddle-wheels and molecular paddle-wheels in SSICs. Cation motion in molecular paddle-wheels often occurs through hopping, but the motion is diffusive in electronic paddle-wheels. Despite this difference, we expect the analogy between electronic and molecular paddle-wheels to be useful, such that many of the concepts developed for molecular paddle-wheels may be transferable to electronic paddle-wheels in monatomic SSICs.

To summarize, our molecular simulations suggest that the SSIC AgI exhibits hidden electronic disorder, and this dynamic electronic disorder leads to electronic paddle-wheels — anion lone pair rotations that couple to cation diffusion. Electronic paddle-wheels may explain important mysteries about conduction mechanisms of SSICs composed of monatomic ions. For example, collective Ag^+ diffusion was recently identified using topological analysis²². Our proposed diffusion mechanism involving lone pair rotations is consistent with this collective diffusion and provides an electronic origin for these collective dynamics. We also anticipate that the cation-anion coupling due to electronic paddle-wheels may be responsible for the anharmonic coupling observed in spectroscopy¹⁵, similar to anharmonic couplings observed in molecular plastic crystals²³.

The ionic diffusion mechanism predicted here is analogous to the paddle-wheel motion observed in molecular solid-state electrolytes. We expect that this analogy can be leveraged to adapt our understanding of molecular electrolytes to monatomic electrolytes. As a result, electronic paddle-wheels expand unifying frameworks for crystalline, amorphous, and liquid molecular electrolytes to include SSICs composed of monatomic ions²⁴. Similarly, electronic paddle-wheels naturally expand the concept of frustration in SSICs to include *dynamical electronic frustration* resulting from lone pair rotations, in analogy to the dynamical frustration caused by molecular paddle-wheels^{25,26}. This paddle-wheel mechanism has been leveraged to design better molecular electrolytes^{11,27,28}. Consequently, understanding electronic paddle-wheels will create rational, electronic-scale design principles that leverage the coupling between lone pair rotations and cation diffusion to discover new superionic conductors.

ACKNOWLEDGEMENTS

We acknowledge the Office of Advanced Research Computing (OARC) at Rutgers, The State University of New Jersey for providing access to the Amarel cluster and associated research computing resources that have contributed to the results reported here.

METHODS

We performed Born-Oppenheimer molecular dynamics simulations with Kohn-Sham density functional theory using the CP2K software package employing a hybrid Gaussian and plane wave (GPW) approach for representing electron density²⁹. By doing so, we neglect the fast electronic modes that require a detailed description of quantum dynamics, and instead focus on the slowest electronic modes that are coupled to the motion of the nuclei and most relevant to ion conduction. We employed the molecularly optimized double- ζ with valence polarization (DZVP) basis set³⁰ with cutoffs of 450 Ry for plane wave energy and 60 Ry for the reference grid. Goedecker-Teter-Hutter pseudopotentials compatible with employed basis sets were used to represent core electrons^{31,32}, while the valence electrons were represented explicitly using the Perdew-Burke-Ernzerhof (PBE) generalized gradient approximation to the exchange-correlation functional³³. The \mathbf{k} -point sampling was performed only at the Γ -point. Long-range dispersion interactions were included using Grimme's D3 van der Waals correction³⁴. Our simulations used a $3 \times 3 \times 3$ supercell of a AgI unit cell with edge length 5.0855 Å⁶. Starting structures were equilibrated for at least 50 ps at 100 K and 750 K in the canonical ensemble (NVT) using the canonical velocity rescaling (CSVR) thermostat³⁵. For the calculation of dynamic properties, equations of motion were propagated for 80 ps in the microcanonical ensemble using velocity Verlet integrator with a timestep of 0.5 fs. The last 40 ps of these trajectories were used for the analysis. Maximally localized Wannier functions were obtained by minimizing their spreads within CP2K^{19,36}.

* rick.remsing@rutgers.edu

- [1] J. C. Bachman, S. Muy, A. Grimaud, H.-H. Chang, N. Pour, S. F. Lux, O. Paschos, F. Maglia, S. Lupart, P. Lamp, L. Giordano, and Y. Shao-Horn, *Chemical Reviews* **116**, 140 (2016).
- [2] A. Banerjee, X. Wang, C. Fang, E. A. Wu, and Y. S. Meng, *Chemical Reviews* **120**, 6878 (2020).
- [3] J. Liang, X. Li, K. R. Adair, and X. Sun, *Accounts of Chemical Research* **54**, 1023 (2021).
- [4] K. Tuo, C. Sun, and S. Liu, *Electrochemical Energy Reviews* **6**, 17 (2023).
- [5] A. Fukumoto, A. Ueda, and Y. Hiwatari, *Solid State Ionics* **3-4**, 115 (1981).
- [6] S. Hull, *Reports on Progress in Physics* **67**, 1233 (2004).
- [7] Y. Gao, A. M. Nolan, P. Du, Y. Wu, C. Yang, Q. Chen, Y. Mo, and S.-H. Bo, *Chemical Reviews* **120**, 5954 (2020).
- [8] E. Secco, *Journal of Solid State Chemistry* **96**, 366 (1992).

- [9] C. S. Babu and B. L. Tembe, Chemical physics letters **194**, 351 (1992).
- [10] M. Ferrario, M. L. Klein, and I. R. McDonald, Molecular Physics **86**, 923 (1995).
- [11] Z. Zhang and L. F. Nazar, Nature Reviews Materials **7**, 389 (2022).
- [12] J. G. Smith and D. J. Siegel, Nature communications **11**, 1483 (2020).
- [13] A. Mondal and S. Balasubramanian, The Journal of Physical Chemistry C **120**, 22903 (2016).
- [14] P. Simonnin, M. Sassi, B. Gilbert, L. Charlet, and K. M. Rosso, The Journal of Physical Chemistry C **124**, 10150 (2020).
- [15] T. M. Brenner, C. Gehrman, R. Korobko, T. Livneh, D. A. Egger, and O. Yaffe, Phys. Rev. Mater. **4**, 115402 (2020).
- [16] G. Aeppli, A. V. Balatsky, H. M. Rønnow, and N. A. Spaldin, Nature Reviews Materials **5**, 477 (2020).
- [17] R. C. Remsing and M. L. Klein, Phys. Rev. Lett. **124**, 066001 (2020).
- [18] R. C. Remsing and M. L. Klein, APL Materials **8**, 050902 (2020).
- [19] N. Marzari, A. A. Mostofi, J. R. Yates, I. Souza, and D. Vanderbilt, Rev. Mod. Phys. **84**, 1419 (2012).
- [20] M. L. Klein, I. R. McDonald, and Y. Ozaki, The Journal of Chemical Physics **79**, 5579 (1983).
- [21] E. Rabani, J. D. Gezelter, and B. Berne, The Journal of chemical physics **107**, 6867 (1997).
- [22] R. Sato, K. Akagi, S. Takagi, K. Sau, K. Kisu, H. Li, and S.-i. Orimo, The Journal of Chemical Physics **158**, 144116 (2023).
- [23] R. M. Lynden-Bell and K. H. Michel, Rev. Mod. Phys. **66**, 721 (1994).
- [24] D. J. Siegel, L. Nazar, Y.-M. Chiang, C. Fang, and N. P. Balsara, Trends in Chemistry **3**, 807 (2021).
- [25] N. Adelstein and B. C. Wood, Chemistry of Materials **28**, 7218 (2016).
- [26] B. C. Wood, J. B. Varley, K. E. Kweon, P. Shea, A. T. Hall, A. Grieder, M. Ward, V. P. Aguirre, D. Rigling, E. Lopez Ventura, *et al.*, Philosophical Transactions of the Royal Society A **379**, 20190467 (2021).
- [27] Z. Zhang, H. Li, K. Kaup, L. Zhou, P.-N. Roy, and L. F. Nazar, Matter **2**, 1667 (2020).
- [28] Z. Zhang, P.-N. Roy, H. Li, M. Avdeev, and L. F. Nazar, Journal of the American Chemical Society **141**, 19360 (2019).
- [29] T. D. Kühne, M. Iannuzzi, M. Del Ben, V. V. Rybkin, P. Seewald, F. Stein, T. Laino, R. Z. Khaliullin, O. Schütt, F. Schiffmann, D. Golze, J. Wilhelm, S. Chulkov, M. H. Bani-Hashemian, V. Weber, U. Borštnik, M. TAILLEFUMIER, A. S. Jakobovits, A. Lazzaro, H. Pabst, T. Müller, R. Schade, M. Guidon, S. Andermatt, N. Holmberg, G. K. Schenter, A. Hehn, A. Bussy, F. Belleflamme, G. Tabacchi, A. Glöß, M. Lass, I. Bethune, C. J. Mundy, C. Plessl, M. Watkins, J. VandeVondele, M. Krack, and J. Hutter, The Journal of Chemical Physics **152**, 194103 (2020).
- [30] J. VandeVondele and J. Hutter, The Journal of Chemical Physics **127**, 114105 (2007).
- [31] S. Goedecker, M. Teter, and J. Hutter, Phys. Rev. B **54**, 1703 (1996).
- [32] M. Krack, Theoretical Chemistry Accounts **114**, 145 (2005).
- [33] J. P. Perdew, K. Burke, and M. Ernzerhof, Phys. Rev. Lett. **77**, 3865 (1996).
- [34] S. Grimme, J. Antony, S. Ehrlich, and H. Krieg, The Journal of Chemical Physics **132**, 154104 (2010).
- [35] G. Bussi, D. Donadio, and M. Parrinello, The Journal of Chemical Physics **126**, 014101 (2007).
- [36] G. Berghold, C. J. Mundy, A. H. Romero, J. Hutter, and M. Parrinello, Phys. Rev. B **61**, 10040 (2000).